ARTICLE

Electrochemical Oxidation of Ethylene on Palladium Electrode

Wei-Xing Wu, Ying Wang*

Chemistry Department, Chinese University of Hong Kong, Hong Kong 999077, China

Abstract

The electrochemical oxidation of C_2H_4 is attracting increasing attention due to its vast potential market. The current electrochemical methods rely on the use of redox mediators, which may produce corrosive intermediates, while direct oxidation is still limited by its low activity and selectivity. Herein, we conducted electrochemical studies to obtain mechanistic insights into the benchmark Pd catalyst. The generated Pd(II) could be the active site for C_2H_4 oxidation. By designing the pulse sequence, we found the ratio of strongly and weakly adsorbed C_2H_4 on Pd to be 0.3:1. The result we obtained provides a guideline for the rational design of high-performance C_2H_4 oxidation catalysts.

Keywords: Electrochemical oxidation reaction; C_2H_4; Palladium; Electrochemical epoxidation; Electrocatalysis

1. Introduction

Ethylene is one of the most produced chemicals in the chemical industry, with a global market size of CNY 1122 billion per year [1]. In China, around 40% of ethylene is used to produce ethylene oxide and ethylene glycol, reaching the market sizes of CNY 42 billion [2] and CNY 58 billion [3] in 2020, respectively. The current manufacture of ethylene oxide and ethylene glycol rely on the oxidation of ethylene with oxygen under high temperature (200−300 °C) and high pressure (1−3 MPa) [4,5], which is energy-intensive. Around 5438 MJ of energy is consumed, and 0.9 tons of CO_2 will be released for every ton of ethylene oxide produced [6,7].

With the increasing accessibility of renewable electricity, integrating electrochemical systems to produce chemicals and fuels has attracted more attention in the last two decades [8−12]. Electrochemical oxidation of ethylene is a green and attractive approach. Partial oxidation of ethylene to desired chemicals is challenging due to the uncontrolled yet favored over-oxidation of CO_2 under large positive bias [13−16]. Indirect oxidation with redox mediators has been proved to be efficient for partial oxidation of ethylene [7,13,14,17−19]. Recently, Sargent and co-workers reported the chlorine-mediated electrochemical conversion of ethylene to ethylene oxide at industrially relevant conditions (1 $A \cdot cm^{-2}$) [7]. Such a strategy was inspired by the chlorohydrin process, where the Cl_2 was produced through the electrochemical oxidation of Cl^-. The Cl^- can be recycled through $2Cl^- \rightarrow Cl_2 \rightarrow HClO + Cl^- \rightarrow CH_2ClCH_2OH + Cl^- \rightarrow 2Cl^-$, and NaOH was regenerated at the cathode simultaneously. Similar methods were also adopted by Krtil and Manthiram, using simulated seawater as the source of Cl^- [13,18]. However, the corrosive intermediates, such as chlorine and hypochlorous acid, raise a substantial concern about the capital cost for electrode and electrochemical reactor fabrication.

Direct electrochemical oxidation of ethylene is green and sustainable, with wide product distribution including acetaldehyde [20], ethylene oxide [13], acetic acid [21] and ethylene glycol [22], yet the selectivity and activity are low. The challenges originate from the low polarity, poor nucleophilicity, and low solubility of ethylene. Early work by Bockris and co-workers found that Pd and Au were active for partial oxidation of ethylene while complete combustion of C_2H_4 to CO_2 was observed on Pt, Rh, and Ir in 1 $mol \cdot L^{-1}$ H_2SO_4 at 80 °C [20]. They suggested that the bond strength between metal and C_2H_4 was the deciding factor for partial oxidation vs. complete oxidation [20]. King and

Received 31 May 2022; revised 27 June 2022; accepted 12 July 2022; Available online 13 July 2022

* Corresponding author, Ying Wang, Tel: (852)39433586, E-mail address: ying.b.wang@cuhk.edu.hk.

https://doi.org/10.13208/j.electrochem.2215004

Goodridge then conducted detailed investigations on the ethylene oxidation to acetaldehyde on Pd in the same condition, where several mechanistic pathways were proposed [23]. The most recent progress made by Lum et al. was also made in neutral condition, achieving 80% faradaic efficiency of ethylene-to-ethylene glycol at c.a. 4 $mA \cdot cm^{-2}$ on Au doped Pd catalyst in neutral conditions [22]. The report is encouraging since partial electrochemical oxidation of ethylene with high selectivity can be achieved under mild conditions, which is more economically feasible at device level. The high activity and selectivity were resulted from the tuning of OH* on the surface of Au/Pd [22]. An "activation" process of holding potential at 1.1 V vs. Ag/AgCl in 0.1 $mol \cdot L^{-1}$ $NaClO_4$ on Pd was critical, according to Lum. They hypothesized the "activation" process to the dynamic surface reconstruction of Pd to achieve different coverages of OH* [24–26].

Understanding the electrochemical behavior of Pd to obtain insights into the activation process is essential for the rational design of catalyst for partial oxidation of ethylene. Thus, we carried out systematic studies of ethylene oxidation on the Pd electrode in neutral media. We noticed significant changes in the cyclic voltammogram of Pd in the presence of C_2H_4 compared to that in the N_2 atmosphere. An alternative chemical pathway involving C_2H_4 to reduce Pd(II) was observed, suggesting the active site for C_2H_4 adsorption. By further investigation of the electrochemical reduction process of C_2H_4 on Pd, part of the adsorption of C_2H_4 was found to be reversible on Pd while the rest to be strongly bind to Pd with the ratio of 1:0.3. The strongly bind C_2H_4 may be responsible for the over-oxidation of CO_2. With this in mind, we suggested several directions for designing an ideal C_2H_4 partial oxidation catalyst.

2. Experimental

2.1. Chemical reagents

$NaClO_4$ (reagent grade, Fisher Chemical), NaOH (reagent grade, Aladdin), $HClO_4$ (analytical grade, VWR Chemicals), Pd/C (10%, BDH Laboratory Supplies), $HAuCl_4$ (reagent grade, Aladdin), perfluorosulfonic acid (PFSA) ionomer dispersion (25%, FuelCellStore) were used without further purification. All the solutions were prepared using deionized water (18.2 MΩ cm).

2.2. Electrode fabrication

Pd disk electrode used in mechanism investigation was used as purchased without further treatment. Pd electrode used in bulk electrolysis was fabricated by spray coating method. 10 mg Pd/C with 5w.t.% PFSA was added into 1 mL 2:1 isopropanol-water solution to prepare ink. After 1 h sonication, the ink was spray coated onto carbon paper with 5% PTFE (Toray 060) until a loading of 0.75 $mg \cdot cm^{-2}$ was reached. The as-obtained Pd electrode was used after drying overnight at 30 °C in vacuum dry chamber. To introduce Au into the Pd surface, the Pd electrode was immersed into 1 $mmol \cdot L^{-1}$ $HAuCl_4$ solution for 2 h at 65 °C and was used as a cathode after drying overnight.

2.3. Electrochemical tests

All electrochemical experiments were performed in a three-electrode set-up using a CHI 660e potentiostat (Chenhua, China), with a platinum wire as the counter electrode, a saturated Ag/AgCl electrode (Ida, China) as the reference electrode and a palladium disk electrode (2 mm diameter, Ida, China) as the working electrode. Unless mentioned, 0.1 $mol \cdot L^{-1}$ $NaClO_4$ with pH = 6.7 was used as the electrolyte. Prior to the electrochemical measurement, the palladium electrode was polished with 500 nm and 50 nm Al_2O_3 paste (Ida, China), followed by sonication in an ultrasound bath. C_2H_4 (99.5%, Huate Gas, China) and N_2 (99.95%, Linde, China) were bubbled at 50 standard cubic centimetres per minute (sccm) for 15 min. All the electrochemical experiments were conducted at 25 °C. All electrochemical data was reported versus reversible hydrogen electrode (RHE).

$$E(\mathrm{RHE}) = E(\mathrm{Ag/AgCl}) + 0.199\,\mathrm{V} + 0.0592 \times \mathrm{pH} \quad (1)$$

3. Results and discussion

3.1. Electrochemical behavior of Pd disk electrode

We first investigated the electrochemical behavior of Pd in N_2 saturated condition in 0.1 $mol \cdot L^{-1}$ $NaClO_4$ (pH = 6.7). Fig. 1a shows the cyclic voltammetric curves of a Pd macro-electrode in 10 consecutive cycles at 100 $mV \cdot s^{-1}$. The peaks related to H-UPD (C_0 and A_0) were clearly observed, similar to those in acidic and alkaline conditions (Figure S1) [27,28]. The H-UPD region is generally used in the literature to determine the electroactive surface area of Pd. We noticed that the currents of C_0 and A_0 increased when the upper limit potential was beyond 1.25 V, which might result from the increased surface roughness (Fig. 1b).

Previous literature suggested that alpha-oxide was first formed on the surface of Pd at 0.5 V [27].

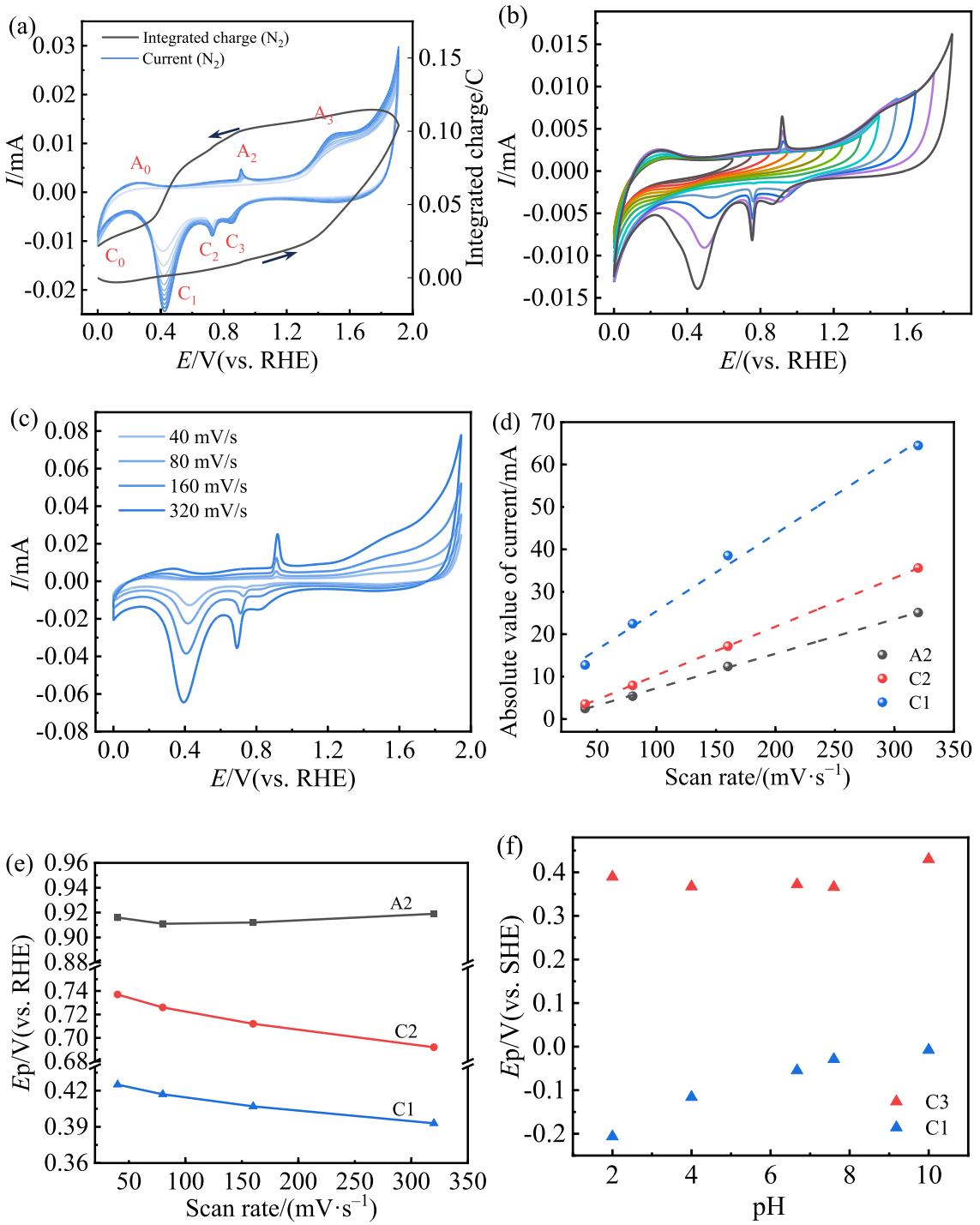

Fig. 1. Electrochemical behavior of Pd in 0.1 mol·L^{-1} $NaClO_4$ under N_2 atmosphere at room temperature: (a) cyclic voltammetric curves in 10 continuous scans at 100 mV·s^{-1}. The right axis shows the charge of the 10th cycle; (b) cyclic voltammetric curves in 13 continuous scans with increasing upper limit potential from 0.65 to 1.85 V vs. RHE; (c) scan-rate voltammetric studies from 40 to 320 mV·s^{-1}; (d) $|I_p|$ vs. scan rate and (e) E_p vs. Ln (scan rate) and (d) pH dependence of C_3 and C_1 peaks at SHE scale (color on line).

This process is kinetically sluggish, giving rise to a barely observable broad peak starting at ca. 0.6 V [27,29]. The alpha-oxide is believed to have a formula of $Pd(OH)_2$ and will form PdO after gradual dehydration [30]. The sharp anodic peak at 0.92 V (A_2) is a surface control process relating to the formation of surface OH* at the step site of Pd (Fig. 1c-d) [31−33]. Additionally, the A_2 only appeared in the second scan when the upper limit potential reached 1.45 V in the previous scan. The current of A_2 increased with the increase of upper limit potential (Fig. 1b). This is related to the

enhanced surface area of Pd from the dissolution-deposition in the electrochemical cycling process, which is consistent with the phenomenon observed in the UPD region. The A_2 peak was not observed at extreme pH (pH = 2 or 12) due to the rapid growth of thick metal oxide layer (Figure S1).

A potential higher than 1.45 V is believed to facilitate the formation of Pd(IV) (A_3), which we assigned as the "harsh" oxidation condition resulting in Pd dissolution [34]. Thus, performing electrochemical cycling of the Pd electrode with an upper limit potential higher than 1.45 V will lead to the dissolution/deposition of the Pd electrode, causing an increase in surface roughness [33,34]. The current enhancement for A_2 and A_0/C_0 after cycling at such potential confirms this statement. The C_3, C_2, and C_1 at 0.84 V, 0.76 V, and 0.42 V, respectively, corresponded to the reduction peaks of A_3, A_2, and A_1, respectively. At C_3, beta-oxide is reduced to alpha-oxide (Pd(IV) → Pd(II)), which is further reduced back to metallic palladium at C_1 (Pd(II) → Pd (0)). C_1 is a proton-coupled electron transfer surface process (Fig. 1e) with a pH dependence feature on the SHE scale (Fig. 1f). The C_3 peak is pH independent (Fig. 1f) but is influenced by the nature of the anion (Figure S2). Vanfsek found that anions were involved in the oxidation of Pd during the transformation of alpha-oxide to beta-oxide in 1 mol·L^{-1} KOH [27]. It is not surprising that the perchlorate anions could participate in the Pd oxidation in a neutral solution due to the low concentration of hydroxide ions. This can explain the pH independent behavior for C_3, in which the perchlorate anions instead of hydroxide would be removed from the PdO_x during reduction. This statement is further confirmed by the earlier onset and lower intensity of A_3/C_3 in 0.1 mol·L^{-1} Na_2SO_4 than those in 0.1 mol·L^{-1} $NaClO_4$, under both N_2 and C_2H_4 atmospheres (Figure S2).

3.2. Electrochemical oxidation of ethylene on Pd

We then investigated the electrochemical behavior of Pd in C_2H_4 atmosphere, with the rest of the conditions identical to N_2 atmosphere. Apparent differences were observed in the presence of C_2H_4 to that in N_2 saturated solution. As shown in Fig. 2a, no peaks were noticed in the UPD region in the presence of C_2H_4, indicating loss of active surface sites for H*. Such effect can be attributed to the stronger adsorption of C_2H_4 than H* on the surface of Pd. Around two folds enhancement was observed for A_2 in C_2H_4 saturated condition than that in N_2. Since the OH* is the precursor for the water oxidation and the oxidation of C_2H_4 [22,34], the enhancement in the

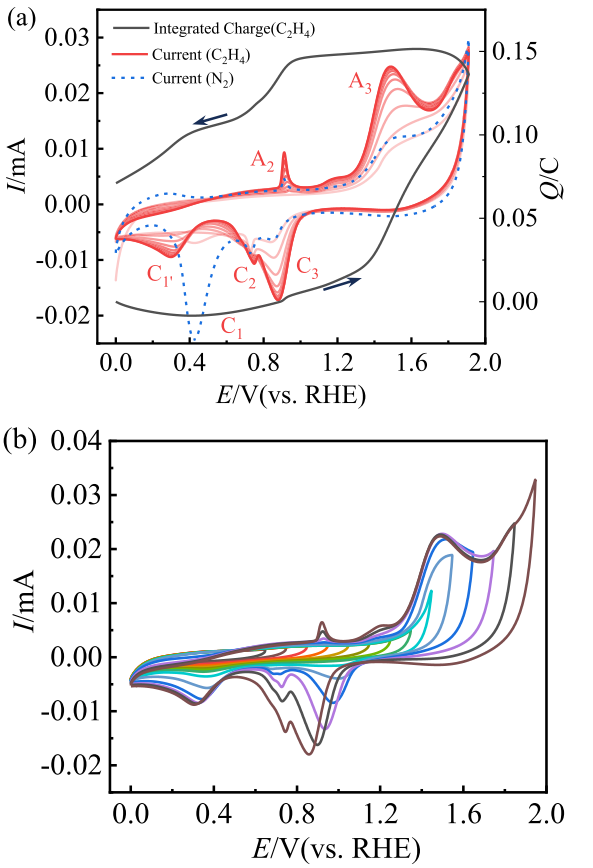

Fig. 2. Electrochemical behavior of Pd in 0.1 mol·L^{-1} $NaClO_4$ under C_2H_4 saturated solution at 100 mV·s^{-1}, room temperature: (a) cyclic voltammetric curves in 10 continuous scans. The right axis shows the charge at the 10th cycle; the dotted blue line is the 10th cycle of CV under N_2 saturated solution, (b) cyclic voltammetric curves in 10 continuous scans with increasing potential upper limit from 0.65 to 1.85 V vs. RHE (color on line).

A_2 implies that the C_2H_4 could be activated by the surface OH* for further oxidation Pd. This is consistent with the observation by Lum et al. [22]. Notable promotion of the current for A_3 and C_3 was observed, related to the oxidation of C_2H_4 or the acceleration of beta oxide growth on Pd.

The C_1 peak (reduction of alpha-oxide) decreased in the continuous scan, accompanied by the appearance of a new peak at 0.3 V, denoted as C_1' (Fig. 2a). At the same time, the C_3 peak was more prominent in the presence of C_2H_4 than that in N_2, while the reduction peak of C_1 was suppressed in the presence of C_2H_4. One possible reason is that there is an alternative chemical reaction pathway to reduce Pd(II) to metallic Pd ($xPd^{2+} + C_2H_4 + 2xOH^- \rightarrow xPd + C_2H_4O_x + xH_2O$), which bypasses the original electrochemical pathway and oxidize C_2H_4 [23]. This could be supported by the larger excess of charge in C_2H_4 saturated solution (0.071 C) than that in N_2 atmosphere (0.021 C) (Figs. 1a and 2a). This also suggests that Pd(II) is the active site for C_2H_4

oxidation. Lum et al. also observed similar behavior in that the fully activated Pd catalyst showed a significant enhancement on C_1 under N_2 atmosphere. Considering that the activation process reported by Lum was performed under 1.1 V vs. Ag/AgCl [22], taken together with what we observed, we propose that the "activation process" might be the promotion of Pd(II) oxide species for optimum adsorption/activation of C_2H_4.

We further designed experiments to investigate different adsorptions of C_2H_4 on Pd. We introduced mechanical perturbation by purging C_2H_4 at 50 sccm to disturb the adsorbed C_2H_4 on the Pd, particularly to remove weakly adsorbed ethylene. As shown in Fig. 3, the disappeared C_1 peak was significantly increased when the mechanical perturbation was introduced (red line in Fig. 3). The C_1 peak disappeared again when the perturbation stopped (blue line), implying the adsorption of C_2H_4 is fast and reversible on Pd. We then suggest that C_1 peak can serve as an indicator to qualitatively characterize the population of adsorbed C_2H_4 on the surface of Pd.

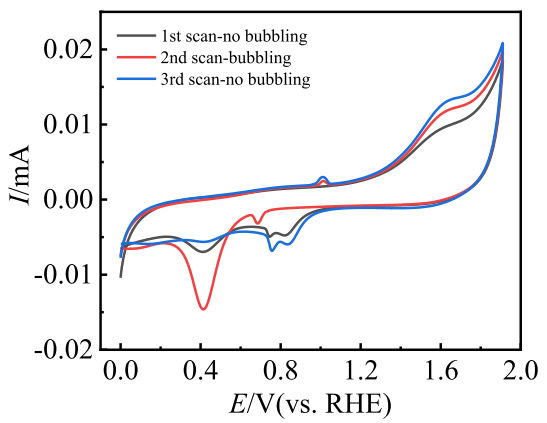

Fig. 3. Cyclic voltammetric curves of Pd in 0.1 mol·L^{-1} $NaClO_4$ under ethylene atmosphere, the bubbling conditions were performed by purging ethylene at 50 sccm (color on line).

We designed pulse sequences (Fig. 4a) to estimate the differently adsorbed C_2H_4 on Pd using C_1 as the indicator. As shown in Fig. 4a, a CV was first performed under ethylene atmosphere (denoted as the before-stripping cycle), followed by holding an anodic potential at 0.9 V for 10 min to allow complete adsorption of C_2H_4. N_2 was then bubbled into the solution for 20 min to replace all the ethylene in the solution. The Pd electrode was held at 0.9 V. This process aimed to remove any weakly adsorbed C_2H_4 on the electrode surface. Two continuous CV cycles were performed (denoted as stripping and after-stripping cycles) afterwards. Control experiments were conducted with all three cycles recorded under N_2 atmosphere (Fig. 4c). The CVs were normalized to the electrochemical active surface area obtained from the capacitance in non-faradic region (Figure S3).

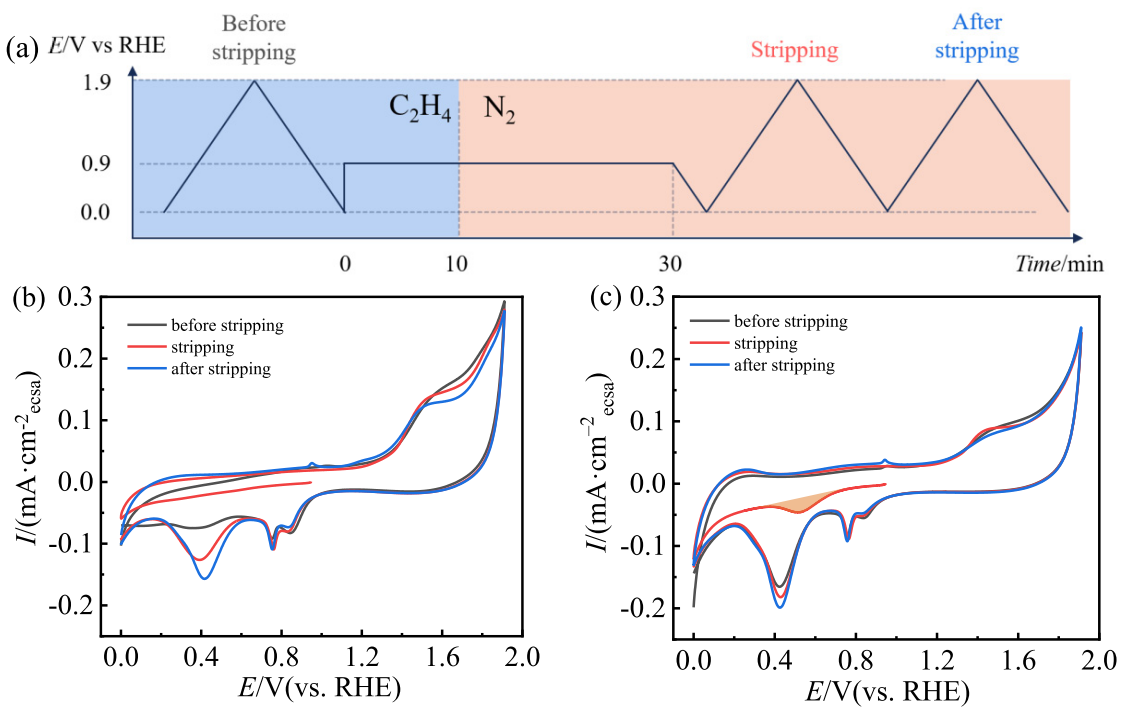

Fig. 4. Ethylene stripping experiment on Pd in 0.1 mol·L^{-1} $NaClO_4$: (a) potential profile of the stripping experiment; (b) cyclic voltammetric tests performed following the pulse condition in (a); (c) control experiments following (a) with N_2 saturated all the time (color on line).

C_1 was not shown in the first segment of the stripping (red line in Fig. 4b), while it was observed in the control experiment (red line in Fig. 4c). At the same time, the peaks in the H-UPD region disappeared in the stripping cycle (red line in Fig. 4b). Considering the previously discussed, it is reasonable to attribute such behavior to the adsorption of ethylene on the surface of Pd. We assigned these C_2H_4 survived from the N_2 bubbling as the strongly adsorbed form, and the population can be estimated based on the charge difference in the 1st segment of the stripping in Fig. 4b and c (shown in the orange shades in Fig. 4c). The intensity of C_1 gradually returned to that in N_2 saturated condition in the consecutive scan, indicating gradual removal of adsorbed C_2H_4 to a complete C_2H_4 free surface (blue line in Fig. 4b). The difference in the charge for C_1 in the after-stripping cycle and before-stripping cycle gives a rough estimation of the C_2H_4 coverage, including both "strongly adsorbed" and weakly adsorbed (based on the charge difference (Q_2) of C_1 in the blue line and the (C_1+$C_{1'}$) in dark line in Fig. 4b). The ratio of strongly adsorbed/weakly adsorbed C_2H_4 is estimated to be 0.3:1 based on $Q_{orange}/(Q_2-Q_{orange})$. The strongly adsorbed C_2H_4 may imply partial oxidation at low positive bias and leads to over-oxidation to CO_2 at large positive potential.

Considering the above discussion and previous works by Cheng [14] and Chorkendorff [15], the partial oxidation of C_2H_4 and even other hydrocarbon species does not simply rely on the *OH on Pd surface. The property of the active site is crucial. Pd is favored for C_2H_4 adsorption, while the partial oxidation pathway might be hindered by the strong bonding of C_2H_4 on the Pd. Thus, surface engineering strategies on the active sites for a balanced C_2H_4 adsorption are useful for future catalyst design. We suggest to introduce metal with weak adsorption to O or C_2H_4 to improve the stability of Pd(II) center and to tune the adsorption of OH* to C_2H_4 for direct partial-oxidation of C_2H_4. To verify our hypothesis, we introduced Au, a noble metal with poor affinity to O [35], into the Pd surface by galvanic exchange reaction. Bulk electrolysis was conducted on both Pd and Pd/Au catalysts at identical conditions (1.7 V vs. RHE, 0.1 mol·L^{-1} $NaClO_4$ electrolyte (pH = 6.7)) and the result is shown in Figure S4. The faradaic efficiencies of ethylene oxide and ethylene glycol increased 50 times on Au/Pd than on Pd, indicating a much improved selectivity to ethylene partial oxidation.

4. Conclusions

In conclusion, we conducted mechanistic studies on the electrochemical oxidation of C_2H_4 on Pd electrode in a neutral solution. Notable differences in the cyclic voltammetric study were found on Pd in N_2 and C_2H_4 atmospheres. The peak relating to Pd(II) reduction was suppressed and evolved towards a more negative bias, indicating an alternative chemical reduction pathway to reduce Pd(II) to Pd (0) in the presence of C_2H_4 and the interaction between Pd(II)-C_2H_4. Further analysis suggested the existence of strongly adsorbed C_2H_4 on Pd, which is around 23%. These strongly adsorbed C_2H_4 might be the reason for the complete combustion of CO_2 under high positive bias.

Acknowledgments

W.W. and Y.W. acknowledge the support of the Research Grants Council of the Hong Kong Special Administrative Region (project no. 24304920).

References

[1] Ethylene Market Size, Share & Covid-19 Impact Analysis, by Application (High-density Polyethylene, Low-Density Polyethylene, Ethylene Oxide, Ethyl Benzene, and Others), and Regional Forecast, 2020-2027[R]. Fortune Business Insights, 2020. Report no.: FBI104532.
[2] 2022-2027年中国环氧乙烷行业市场全景评估及发展战略规划报告[R]. 华经产业研究院, 2022. Report no.: 791393.
[3] 2022-2028年中国乙二醇行业市场深度分析及未来趋势预测报告[R]. 智研咨询, 2022. Report no.: R982367.
[4] Pu T, Tian H, Ford M E, Rangarajan S, Wachs I E. Overview of selective oxidation of ethylene to ethylene oxide by Ag catalysts[J]. ACS Catal., 2019, 9(12): 10727−10750.
[5] Pinaeva L G, Noskov A S. Prospects for the development of ethylene oxide production catalysts and processes (review) [J]. Petrol. Chem., 2020, 60(11): 1191−1206.
[6] Boulmanti A, Moya J A. Energy efficiency and GHG emissions: Prospective scenarios for the chemical and petrochemical industry[R]. Luxembourg. Publications Office of the European Union, 2017. EUR 28471 EN. https://doi.org/10.2760/20486.
[7] Leow W R, Lum Y, Ozden A, Wang Y H, Nam D H, Chen B, Wicks J, Zhuang T T, Li F W, Sinton D, Sargent E H, Sargent. Chloride-mediated selective electrosynthesis ofethylene and propylene oxides at high current density[J]. Science, 2020, 368(6469): 1228−1233.
[8] Li R, Xiang K, Peng Z K, Zou Y Q, Wang S Y. Recent advances on electrolysis for simultaneous generation of valuable chemicals at both anode and cathode[J]. Adv. Energy Mater., 2021, 11(46): 2102292.
[9] Na J, Seo B, Kim J, Lee C W, Lee H, Hwang Y J, Min B K, Lee D K, Oh H S, Lee U. General technoeconomic analysis for electrochemical coproduction coupling carbon dioxide reduction with organic oxidation[J]. Nat. Commun., 2019, 10(1): 5193.
[10] Li T F, Cao Y, He J F, Berlinguette C P. Electrolytic CO_2 reduction in tandem with oxidative organic chemistry[J]. ACS Cent. Sci., 2017, 3(7): 778−783.
[11] Xie Y A, Zhou Z Y, Yang N J, Zhao G H. An overall reaction integrated with highly selective oxidation of 5-hydroxymethylfurfural and efficient hydrogen evolution[J]. Adv. Funct. Mater., 2021, 31(34): 2102886.
[12] Wang T H, Tao L, Zhu X R, Chen C, Chen W, Du S Q, Zhou Y Y, Zhou B, Wang D D, Xie C, Long P, Li W,

Wang Y Y, Chen R, Zou Y Q, Fu X Z, Li Y F, Duan X F, Wang S Y. Combined anodic and cathodic hydrogen production from aldehyde oxidation and hydrogen evolution reaction[J]. Nat. Catal., 2022, 5(1): 66−73.

[13] Chung M, Jin K, Zeng J S, Manthiram K. Mechanism of chlorine-mediated electrochemical ethylene oxidation in saline water[J]. ACS Catal., 2020, 10(23): 14015−14023.

[14] Hong J C, Kuo T C, Yang G L, Hsieh C T, Shen M H, Chao T H, Lu Q, Cheng M J. Atomistic insights into Cl^--Triggered highly selective ethylene electrochemical oxidation to epoxide on RuO_2: unexpected role of the *in situ* generated intermediate to achieve active site isolation[J]. ACS Catal., 2021, 11(21): 13660−13669.

[15] Winiwarter A, Silvioli L, Scott S B, Enemark-Rasmussen K, Sariç M, Trimarco D B, Vesborg P CK, Moses P G, Stephens I EL, Seger B, Rossmeisl J, Chorkendorff I. Towards an atomistic understanding of electrocatalytic partial hydrocarbon oxidation: propene on palladium[J]. Energy Environ. Sci., 2019, 12(3): 1055−1067.

[16] Sebera J, Hoffmannova H, Krtil P, Samec Z, Zalis S. Electrochemical and density functional studies of the catalytic ethylene oxidation on nanostructured Au electrodes[J]. Catal. Today, 2010, 158(1−2): 29−34.

[17] Xu L P, Xie Y, Li L J, Hu Z F, Wang Y, Yu J C. Highly selective photocatalytic synthesis of ethylene-derived commodity chemicals on biobr nanosheets[J]. Mater. Today Phys., 2021, 21: 100551.

[18] Jirkovsky J S, Busch M, Ahlberg E, Panas I, Krtil P. Switching on the electrocatalytic ethene epoxidation on nanocrystalline RuO_2[J]. J. Am. Chem. Soc., 2011, 133(15): 5882−5892.

[19] Schalck J, Hereijgers J, Guffens W, Breugelmans T. The bromine mediated electrosynthesis of ethylene oxide from ethylene in continuous flow-through operation[J]. Chem. Eng. J., 2022, 446(2): 136750.

[20] Dahms H, Bockris J O'M. The relative electrocatalytic activity of noble metals in the oxidation of ethylene[J]. J. Electrochem. Soc., 1964, 111(6): 728.

[21] Blake A R, Sunderland J G, Kuhn A T. The partial anodic oxidation of ethylene on palladium[J]. J. Chem. Soc. A 1969: 3015−3018.

[22] Lum Y, Huang J E, Wang Z, Luo M, Nam D H, Leow W R, Chen B, Wicks J, Li Y C, Wang Y, Dinh C T, Li J, Zhuang T T, Li F, Sham T K, Sinton D, Sargent E H. Tuning OH binding energy enables selective electrochemical oxidation of ethylene to ethylene glycol[J]. Nat. Catal., 2020, 3(1): 14−22.

[23] Goodridge CJHK F. Oxidation of ethylene at a palladium electrode[J]. Trans. Faraday Soc., 1970, 66: 2889−2896.

[24] Triaca W E, Castroluna A M, Arvia A J. The electrocatalytic oxidation of ethylene on platinized platinum at different saturation pressures[J]. J. Electrochem. Soc., 1980, 127(4): 827−833.

[25] Boyd M J, Latimer A A, Dickens C F, Nielander A C, Hahn C, Norskov J K, Higgins D C, Jaramillo T F. Electrooxidation of methane on platinum under ambient conditions[J]. ACS Catal., 2019, 9(8): 7578−7587.

[26] Spendelow J S, Goodpaster J D, Kenis P JA, Wieckowski A. Mechanism of Co oxidation on Pt(111) in alkaline media[J]. J. Phys. Chem. B, 2006, 110(19): 9545−9555.

[27] Birss V I, Beck V H, Zhang A J, Vanysek P. Properties of thin, hydrous Pd oxide films[J]. J. Electroanal. Chem., 1996, 429(1−2): 175−184.

[28] Jaksic M M, Johansen B, Tunold R. Electrochemical-behavior of palladium in acidic and alkaline-solutions of heavy and regular water[J]. Int. J. Hydrogen Energy, 1993, 18(2): 111−124.

[29] Chierchie T, Mayer C, Lorenz W J. Structural changes of surface oxide layers on palladium[J]. J. Electroanal. Chem., 1982, 135(2): 211−220.

[30] Grden M, Lukaszewski M, Jerkiewicz G, Czerwinski A. Electrochemical behaviour of palladium electrode: oxidation, electrodissolution and ionic adsorption[J]. Electrochim. Acta, 2008, 53(26): 7583−7598.

[31] Dall'Antonia L H, remiliosi-Filho G, Jerkiewicz G. Influence of temperature on the growth of surface oxides on palladium electrodes[J]. J. Electroanal. Chem., 2001, 502(1−2): 72−81.

[32] Sashikata K, Matsui Y, Itaya K, Soriaga M P. Adsorbed-iodine-catalyzed dissolution of Pd single-crystal electrodes: studies by electrochemical scanning tunneling microscopy [J]. J. Phys. Chem., 1996, 100(51): 20027−20034.

[33] Perdriel C L, Custidiano E, Arvia A J. Modifications of palladium electrode surfaces produced by periodic potential treatments[J]. J. Electroanal. Chem., 1988, 246(1): 165−180.

[34] Juodkazis K, Juodkazyte J, Sebeka B, Stalnionis G, Lukinskas A. Anodic dissolution of palladium in sulfuric acid: an electrochemical quartz crystal microbalance study [J]. Russ. J. Electrochem., 2003, 39(9): 954−959.

[35] Hammer B, Norskov J K. Why gold is the noblest of all the metals[J]. Nature, 1995, 376(6537): 238−240.

乙烯在钯圆盘电极的电化学氧化研究

吴炜星，王　莹*
香港中文大学化学系，香港 999077，中国

摘要

由于巨大的潜在市场，乙烯的电化学氧化受到愈来愈多的关注。目前，主流的电化学氧化法仍以依赖于氧化还原媒介的介导氧化法为主，而这些媒介的使用在电解过程中产生大量的腐蚀性中间体，使其实际应用受到阻碍。直接电氧化法可有效规避此问题，但又受到低活性和低选择性的限制。在本工作中，我们针对目前最先进的钯催化直接氧化体系，在中性条件下开展了一系列电化学研究，以对该过程的机理获取更深入的认识。在氮气和乙烯氛围下，钯电极的循环伏安谱图有显著区别。我们发现电解过程中生成的 Pd(II)物种在乙烯氛围下可绕过原本的电化学还原路径，通过一个化学步还原为 Pd(0)，因此可能是乙烯氧化的活性位点。Pd(II)物种所对应的还原峰也因此可作为乙烯吸附的数量的指标。通过电化学脉冲序列的设计，我们在钯催化剂上识别了两种具有不同吸附强度的乙烯，其强、弱吸附模式所对应的电荷转移比例约为 0.3:1。弱吸附的乙烯在钯电极表面表现出可逆的吸脱附行为，而具有强吸附模式的乙烯无法通过物理过程脱附，可能指向到乙烯深度氧化过程。这项工作为进一步设计高性能乙烯直接电氧化催化剂提供了设计思路和方向。

关键词：电氧化反应；乙烯；吸附；钯；电环化反应